EClinicalMedicine 39 (2021) 101058

Contents lists available at ScienceDirect

EClinicalMedicine

journal homepage: https://www.journals.elsevier.com/eclinicalmedicine

Research Paper

Impact of residual thrombus burden on ventricular deformation after acute myocardial infarction: A sub-analysis from an intravascular optical coherence tomography study

Jinying Zhou[a,#], Shiqin Yu[a,#], Peng Zhou[a,b], Chen Liu[a,b], Zhaoxue Sheng[a], Jiannan Li[a], Runzhen Chen[a], Hongbing Yan[a,b,a,*], Shihua Zhao[a]

[a] Fuwai Hospital, National Center for Cardiovascular Diseases, Chinese Academy of Medical Sciences and Peking Union Medical College, Beijing, China
[b] Fuwai Hospital, Chinese Academy of Medical Sciences, Shenzhen, China

ARTICLE INFO

Article History:
Received 9 May 2021
Revised 12 July 2021
Accepted 14 July 2021
Available online xxx

Keywords:
ST elevation myocardial infarction
Thrombosis
Optical coherence tomography
Cardiac magnetic resonance
ventricular function

ABSTRACT

Background: Coronary residual thrombus before stenting in ST-segment elevation myocardial infarction (STEMI) has been linked to microvascular injury but its impact on ventricular deformation and cardiac dysfunction in longer term remains unclear.

Methods: This was a post-hoc sub-analysis from an optical coherence tomography registry. Residual thrombus before stenting was measured geometrically and maximal thrombus-to-lumen area ratio (MTR) was reported. Cardiovascular magnetic resonance (CMR) follow-ups were performed at 30 days post STEMI. The primary outcomes were CMR-derived parameters including left ventricular ejection fraction (LVEF), infarct size, microvascular obstruction (MVO), and left ventricular global strains in radial (GRS), circumferential (GCS), longitudinal (GLS) directions.

Findings: From March 2017 to March 2019, forty-two patients with first-ever anterior STEMI were included. Average CMR follow-up time was 33 (IQR 30–37) days. In multivariable analysis, MTR was significantly associated with LVEF (per 10%, adjusted β = -1·96, 95%CI -3·66 to -0·26), MVO (per 10%, adjusted β = 0·07, 95%CI 0·01 to 0·13), GRS (per 10%, adjusted β = -1·26, 95%CI -2·28 to -0·23), and GCS (per 10%, adjusted β = 0·53, 95%CI 0·01 to 1·06). However, it was not related to GLS (per 10%, adjusted β = 0·29, 95%CI -0·85 to 1·43) or infarct size (per 10%, adjusted β = 0·07, 95%CI -0·40 to 0·55).

Interpretation: Larger residual thrombus burden was associated with worse GRS and GCS but not GLS after a first anterior myocardial infarction.

Funding: This work was supported by Chinese Academy of Medical Sciences Innovation Fund for Medical Sciences (2016-I2M-1–009), National Natural Science Foundation of China (81,970,308, 81,930,044, and 81,620,108,015), Sanming Project of Medicine in Shenzhen (SZSM201911017), and Shenzhen Key Medical Discipline Construction Fund (No. SZXK001).

1. Introduction

Despite successful recanalization of epicardial coronary, a group of patients with ST-segment elevation myocardial infarction (STEMI) suffer from sustained myocardial ischemia [1,2]. Thrombus fragments and plaque debris could induce microvascular obstruction (MVO) [3,4] and contribute to adverse clinical outcomes [5]. However, large randomized trials [6–8] did not show improved clinical outcomes from routine thrombus aspiration. To note, a previous optical coherence tomography study showed that additional manual thrombectomy failed to reduce more thrombus than intervention alone [9]. Moreover, Higuma et al. reported that residual thrombus burden after aspiration thrombectomy had an impact on post-procedural myocardial damage [10]. However, it remains unclear whether residual thrombus burden before stenting has an impact on short-term myocardial deformation.

Heart failure after acute myocardial infarction remains a common and major healthcare burden. Improvement in left ventricular (LV) systolic function, specifically indicated by LV ejection fraction (LVEF), is widely recognised as an indicator of treatment effects and a surrogate for clinical outcome. However, several studies suggested that

* Corresponding authors. Hongbing Yan, MD, PhD, No.167, North Lishi Road, Xicheng District, Beijing, 100037, China.
E-mail addresses: hbyanfuwai2018@163.com (J. Zhou), hbyanfuwai2018@163.com (H. Yan), cjrzhaoshihua2009@163.com (S. Zhao).
# Drs. Jinying Zhou and Shiqin Yu contributed equally to this study.

https://doi.org/10.1016/j.eclinm.2021.101058

Research in context

Evidence before this study

Routine thrombus aspiration during primary percutaneous coronary intervention failed to improve clinical outcomes in patients with acute myocardial infarction. However, intravascular imaging studies showed significant impact of residual thrombus burden on post-procedural myocardial damage and microvascular dysfunction.

Added value of this study

The adverse impact of large residual thrombus burden persisted over the one-month acute phase after myocardial infarction. In patients with a first-ever anterior ST-segment elevation myocardial infarction, maximal thrombus-to-lumen area ratio reflected residual thrombus burden well and had independent prognostic value.

Implications of all the available evidence

Attentions should be paid to the non-neglectable and persistent impact of residual thrombus on ventricular deformation after myocardial infarction. Therefore, more efficient methods other than thrombus aspiration are clearly warranted investigation.

failure in LVEF improvement was not associated with subsequent death after revascularization treatments [11,12]. On the other hand, late gadolinium enhancement (LGE) imaging by cardiovascular magnetic resonance (CMR) provides qualification of infarct size after myocardial infarction [13,14], which has been another independent predictor for clinical outcomes [15-17]. LV strain by CMR feature tracking (CMR-FT) analysis is an emerging approach for myocardial deformation and could be a sensitive marker of ventricular deformation [18].

Thus, this study aimed to investigate whether residual thrombus burden before stenting is associated with short-term LV deformation in patients with first-ever anterior STEMI after primary percutaneous coronary intervention (PPCI).

2. Methods

2.1. Participants and setting

This is a sub-analysis of the OCTAMI (Optical Coherence Tomography Examination in Acute Myocardial Infarction) registry (NCT03593928), which prospectively enrolled consecutive STEMI patients at the institution hospital and evaluated coronary culprit lesions with OCT. Major inclusion criteria for the OCTAMI registry were age ≥18 years and diagnosis of STEMI [19] (details in supplemental materials). Participation in this sub-study required a diagnosis of first-ever anterior STEMI and patient's informed consent to a CMR follow-up (Fig. 1). In addition to the exclusion criteria of the OCTAMI registry, patients were excluded from this sub-study if they had previous stent implantation, or contradictions to CMR. The study complied with principles of the Declaration of Helsinki and was approved (No.2017−866) by the institution review board and was reported according to the STrengthening Reporting of OBservational studies in Epidemiology (STROBE) guidelines [20].

2.2. Procedural data and OCT imaging

All patients received standard care according to international guidelines [19,21]. Baseline LVEF was measured at admission by

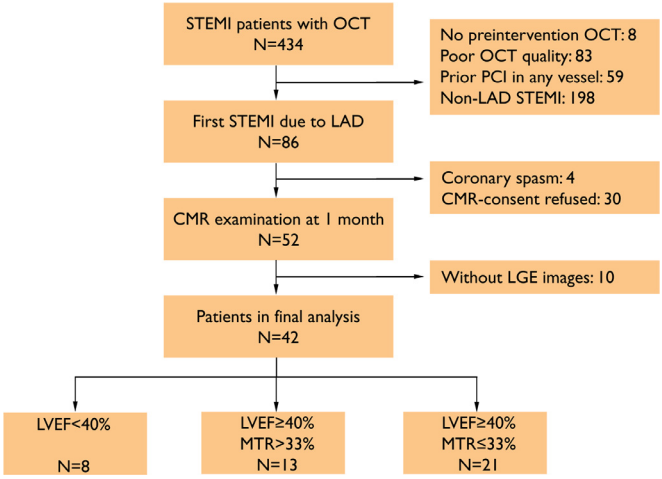

Fig. 1. Study flow, CMR = cardiovascular magnetic resonance; LAD = left anterior descending artery; LGE = late gadolinium enhancement; LVEF = left ventricular ejection fraction; MTR = maximal thrombus-to-lumen ration; PCI = percutaneous coronary intervention; OCT = optical coherence tomography; STEMI = ST-segment elevated myocardial infarction.

echocardiography. The culprit vessel was determined primarily by coronary angiography and corroborated with electrocardiogram and echocardiographic information. OCT examinations were performed as previously reported [22−24]. Briefly, the frequency-domain OCT system (ILUMIEN OPTIS™, St. Jude Medical/Abbott, St. Paul, MN, USA) and a dragonfly catheter (Lightlab Imaging, Inc., Westford, MA, USA) were applied under a TIMI grade 3 flow condition. For restoration of antegrade blood flow, aspiration was used up to the operator.

2.3. OCT image analysis

OCT image analysis was consistent with previous analyses from OCTAMI registry [22,23]. Definitions of OCT characteristics were based mainly on established consensus [25] and details were in supplemental materials. Thrombus was defined as an irregular mass floating in the lumen or adjacent to the luminal surface. Representative samples are shown in Fig. 2. Lumen area (Fig. 2b) and thrombus area (Fig. 2d) were both measured by planimetry per frame. Total residual thrombus volume or total lumen over 30 mm measurable length were reported, respectively, and their ratio was reported as total thrombus-to-lumen volume ratio (TTR). Maximal thrombus-to-lumen area ratio (MTR) per frame within 30 mm measurable length was reported. Flow area (Fig. 2c) was calculated by subtracting residual thrombus area (if any) from lumen area per frame and the minimal flow area (MFA) was reported.

2.4. CMR imaging protocol

CMR imaging was performed on a 3·0-Tesla scanner (Discovery MR750, GE Healthcare, Milwaukee, USA) with a phased-array cardiovascular coil, using electrocardiographic and respiratory gating. LV cine images were acquired in 3 long-axis views (two-chamber, four-chamber, and outflow tract) and series of short-axis views encompassing the entire LV using balanced steady state free precession sequence (b-SSFP). LGE images were acquired 10 to 15 min after intravenous administration of gadolinium-DTPA (Magnevist, Bayer, Berlin, Germany) at a dose of 0·2 mmol/kg, using a segmented phase-sensitive inversion recovery Turbo Fast Low Angle Shot sequence at the same views as cine images in end diastole.

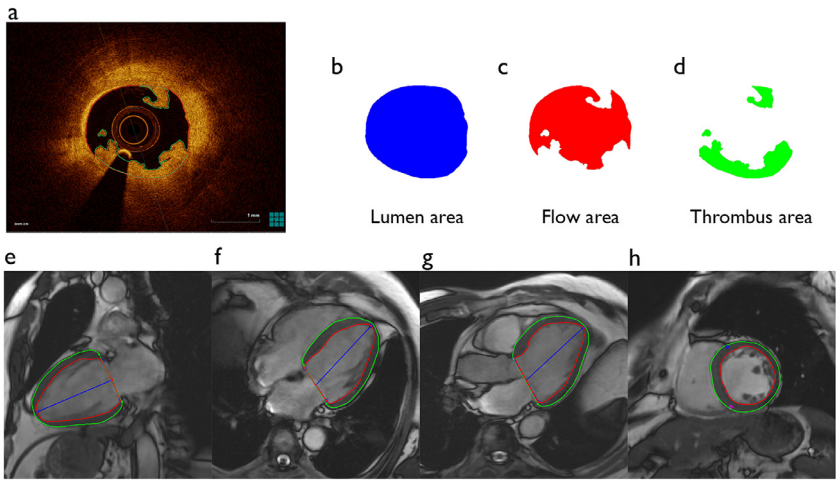

Fig. 2. Measurements of residual thrombus on OCT and LV strain by cardiovascular magnetic resonance-Feature tracking, A representative frame of OCT image (a) and measurements including lumen area (b), flow area (c), and thrombus area (d). Left ventricular endo- and epicardial contours were manually delineated at the phase of end-diastole on the 2-chamber (e), 4-chamber (f), outflow tract (g), and short axis (h) cine images, respectively. OCT = optical coherence tomography.

2.5. CMR analysis

All CMR images were analysed using CVI42 (Circle Cardiovascular Imaging Inc., Calgary, Canada) by two radiologists with 3- and 5-year experience of CMR imaging, respectively. Endocardial and epicardial contours of left ventricular myocardium were manually traced on short-axis cine images at end diastole and end systole respectively, and papillary muscles were assigned to the LV volume. LV volumetric and functional parameters were automatically computed. Infarct size was determined by the presence of contrast enhancement on LGE imaging was detected by +5 SDs over the signal intensity of normal myocardium. The CMR-FT analysis were performed on b-SSFP cine images and all endocardial and epicardial borders of LV were manually delineated at end diastole (Fig. 2e-f) and automatically tracked throughout cardiac cycle with manual adjustment if necessary. Short-axis cine images were tracked to derive radial and circumferential strains while long-axis cine images were delineated to calculate longitudinal strain. LV global peak radial (GRS), circumferential (GCS), and longitudinal (GLS) strains were reported. LV segmental peak strains in accordance with American Heart Association 16-segment model were also reported in radial, circumferential, and longitudinal directions. For inter-observer reproducibility evaluation, a randomly selected set of ten patients were independently assessed by the two investigators. One of the investigators repeated the measurement 1 month later to determine the intra-observer variability. Inter-observer and intra-observer reproducibility were reported in eTable 3.

2.6. Statistical analysis

Missing data and cleaning methods were summarized in eTable1. Categorical variables were reported as frequency (%) and compared by $\chi 2$ test or Fisher exact. Continuous variables with normal distributions were reported as mean and SD while those deviating from normal distributions as median and IQR. Continuous variables were compared using independent-sample *t*-test, Mann-Whitney test, ANOVA, or Kruskal-Wallis H as appropriate. Bivariate correlations were assessed by Pearson correlation coefficient or Spearman rank correlation coefficient as appropriate. Simple linear regression analysis between each residual thrombus burden parameters and each primary outcome were tested. For adjustments in multivariable regression analysis, we adapted a two-step strategy. In the first step, we performed univariable linear regression analyses for each CMR outcome on each baseline variable to select those with two-sided p values <0·1 to go into multivariable linear regression models. Second, we additionally adjusted for age and sex. Covariates included in each multivariable models were reported in the footnote. ROC analysis was used to determine the optimal threshold of MTR for predicting LV dysfunction at 30-day follow-up. Group comparisons were carried out using default method from the R package *compareGroups* v4·4·5 [26]. The intraclass correlation coefficient from two-way random effects model was used to assess the inter- and intra-observer variability. All analyses were performed using SPSS Statistics 24·0 software (IBM Corp, Armonk, NY) and R software, version 4·0·3 (R Foundation for Statistical Computing, Vienna, Austria).

2.7. Role of funding sources

The funders had no role in the conduct or report of the research.

3. Results

3.1. Baseline clinical features, OCT measurements, and follow-up CMR parameters

Analysable pre-stenting OCT images were acquired in 86 patients with a first anterior STEMI. Finally, 42 patients were included in current analysis (Fig. 1) and the time of CMR follow-up was 33 (IQR 30−37) days. Comparisons of baseline characteristics between included and excluded population were reported in eTable2.

As shown in Table 1, the average age was 54 years old and 37 out of 42 patients were male. OCT examinations showed that 25 (59·5%) patients presented plaque rupture. The median TTR was 0·9%, the median MFA was 1·02 mm^2, and the average MTR was 31·3%. Distribution of MTR was reported in eFig. 1. CMR follow-up results were summarised in Table 2. The average LV global peak strains of the entire group were 23·3%, −14·6%, and −12·1% in radial, circumferential, and longitudinal directions, respectively, with references of 37·9%, −20·5%, and −15·4%. All LV global peak strain parameters showed good to excellent intra-observer (0·96 to 0·97) and inter-observer (0·94 to 0·96) agreement (eTable 3).

3.2. Association of residual thrombus burden with LV deformation

As shown in eTable 4, MTR was significantly associated with LVEF, MVO percentage, GRS and GCS; TTR was significantly associated with LVEF; while MFA was not significantly associated with any primary outcomes. Paired scatter plots between residual thrombus burden

Table 1
Baseline characteristics of the included population.

	N = 42
Demographics	
Age, years	54·1 ± 8·4
Men, n (%)	37 (88·1)
Body mass index, kg/m	25·9 (24·3, 27·8)
Smoking, n (%)	30 (71·4)
Hypertension, n (%)	20 (47·6)
Diabetes mellitus, n (%)	13 (31·0)
Lab indicators	
Peak cTnI, ng/mL	29·5 (8·7, 51·9)
Peak NT-proBNP, pg/mL	965·0 (605·6, 2227·2)
Hs-CRP, mg/L	5·3 ± 4·3
LDL-C, mg/dL	120·7 ± 33·5
eGFR, ml/min/1·732 m^2	105·0 ± 27·7
Index episode	
Symptom onset, hours	5·0 (3·0, 6·8)
Door to balloon time, mins	108 (82, 149)
LVEF at admission,%	53·9 ± 6·0
Procedure characteristics	
Initial TIMI grade 0–1, n (%)	31 (73·8)
Aspiration, n (%)	30 (71·4)
Stent implantation, n (%)	41 (97·6)
Post dilation, n (%)	32 (78·0)
Glycoprotein IIb/IIIa inhibitor, n (%)	9 (21·4)
Final TIMI grade 3, n (%)	42 (100)
Optical coherence tomography characteristics	
Plaque rupture, n (%)	25 (59·5)
Lipid plaque, n (%)	16 (38·1)
Thin-cap fibroatheroma, n (%)	8 (19·0)
Calcification, n (%)	16 (38·1)
Micro vessels, n (%)	8 (19·0)
Cholesterol crystal, n (%)	2 (4·8)
Macrophage infiltration, n (%)	17 (40·5)
Fibrous cap thickness, μm	90 (70, 108)
Maximal lipid arc, °	342 (231, 360)
Residual thrombus burden	
TTR,%	0·9 (0·4, 2·6)
MTR,%	31·3 ± 14·6
MFA, mm^2	1·02 (0·83, 1·39)

Values are mean ± SD, median (IQR), or n (%). cTnI = cardiac troponin I; eGFR = estimated glomerular filtration rate; Hs-CRP = high-sensitivity C-reactive protein; LDL-*C* = low-density lipoprotein cholesterol; LVEF = left ventricular ejection fraction; MFA = minimal flow area; MTR = maximal thrombus-to-lumen ratio; NT-proBNP = *N* terminal pro B type natriuretic peptide; TIMI = thrombolysis in myocardial infarction; TTR = total thrombus-to-lumen ratio.

parameters and primary outcomes were provided in eFig. 2. In univariable regression analysis, aspiration or not was not associated with LVEF (p = 0.418), infarct size (p = 0.426), MVO (p = 0.410), GRS (p = 0.927), GCS (p = 0.837), and GLS (p = 0.851). Covariates included in first-step multivariable models for each CMR parameter were: 1) for LVEF: peak cardiac troponin I (cTnI), peak N-terminal pro b-type natriuretic peptide (NT-proBNP), high-sensitivity C-reactive protein (Hs-CRP), and LVEF at admission; 2) for infarct size: peak cTnI, peak NT-proBNP, Hs-CRP, estimated glomerular filtration rate (eGFR), and LVEF at admission; 3) for MVO: peak cTnI and LVEF at admission; 4) for GRS: peak cTnI, low density lipoprotein cholesterol (LDL-C), Hs-CRP, and LVEF at admission; 5) for GCS: peak cTnI, Hs-CRP, and LVEF at admission; 6) for GLS: peak cTnI and LVEF at admission. After these adjustments, the predictive value of MTR for LVEF, MVO percentage, GRS and GCS was preserved. However, neither TTR nor MTR were independent predictors for infarct size (Table 3). Additional adjustment for age and sex showed similar results (Table 3).

3.3. MTR and LV deformation in patients without severely impaired LVEF

ROC analysis was performed to obtain the optimal threshold of MTR in predicting left ventricular dysfunction at 30 days after the index event. Sensitive analysis was performed by using different

Table 2
Primary outcomes: left ventricular deformation and dysfunction assessed by CMR at 30 days.

	Study group *N* = 42
Primary outcomes	
LVEF,%	50·7 ± 10·7
Infarct size,%	10·4 (4·3, 17·1)
MVO presence	25 (59·5)
MVO percentage,%	0·5 (0·0, 1·0)
Left ventricular global peak strain	
GRS,%	23·3 ± 6·4
GCS,%	−14·6 ± 3·1
GLS,%	−12·1 ± 2·4
Other CMR parameters	
Stroke volume, mL	**72·4 ± 19·5**
LVEDVi, mL/m2	**76·3 (68·8, 84·4)**
LVESVi, mL/m2	**37·2 (30·8, 45·6)**
Cardiac output, L/min	**4·5 ± 1·2**
Cardiac index, L/min/m2	**2·4 ± 0·6**

Values are mean ± SD, median (IQR), or n (%). CMR = cardiac magnetic resonance; GCS = global circumferential strain; GLS = global longitudinal strain; GRS = global radial strain; LVEF = left ventricular ejection fraction; LVEDVi = left ventricular end-diastolic volume index; LVESVi = left ventricular end-systolic volume index; MVO = microvascular obstruction.

LVEF cutoffs for defining left ventricular dysfunction and results were shown in eTable 5. The optimal threshold value of MTR was 33.7% for predicting LVEF<50% at 30-day follow-up, with a sensitivity of 75% and a specificity of 77%. Compared across patient with LVEF<40%, patients with LVEF≥40% and MTR≤33%, and patients with LVEF≥40% and MTR>33% (eTable 6), there were significant trend of decline in infarct size while significant trends of improvement in LVEF, GRS, GCS, and GLS. Detailed results of segmental analysis of LGE presence (eTable 7 and eFigure 3A) and segmental strain (eTable 8 and eFigure 3B-D) were in supplementary materials. CMR data from an independent group of anonymous age-and-sex-matched controls were also collected to set reference values for strain analyses (eTable 9). Three representative cases were shown in eFigure 4.

4. Discussion

Our study investigated the association of residual thrombus burden and LV deformation at 30 days in patients with first-ever anterior STEMI after PPCI. The main finding of this study was that larger thrombus burden, indicated by MTR but not TTR or MFA, was associated with worse left ventricular global peak strains in radial and circumferential directions and more MVO at 30-day follow-up. This indicated that an appropriate residual thrombus burden parameter could predicted persistent LV deformation post STEMI.

Accurate in vivo measurement of coronary residual thrombus remains challenging. Previously, angiographical and hemodynamic criteria were used for defining large thrombus budern [27]. Currently, OCT provides both qualitative [28] and quantitative analysis of thrombus (by planimetry [10] or a semi-quantitative thrombus score [29]). Higuma et al. reported the impact of residual thrombus burden on post-procedural microvascular flow and peak creatine kinase MB [10]. Large clinical trials [6–8] failed to show improved prognosis from routine aspiration. However, Bhindi et al. reported that manual thrombectomy did not reduce more thrombus than stenting alone [9]. Thus, we suspected that residual coronary thrombus, even after aspiration, at culprit lesion before stenting could have an impact on final myocardial injury.

Myocardial deformation after STEMI provides incremental prognostic value than LVEF and infarct size [30-32] and previous studies suggested GLS as the strongest prognosticator among strain parameters [31,32]. The current study showed that MTR was significantly associated with GRS and GCS but not GLS. Time of CMR examination

Table 3
Regression analysis for primary outcomes (LVEF, infarct size, MVO, GRS, GCS, and GLS) at 30 days.

For LVEF,%	Crude β	95% CI	p	Adjusted β*	95% CI	p	Adjusted β†	95% CI	p
TTR, per 10%	−12·34	−21·05 to −3·63	<0·01	−8·06	−15·04 to −1·09	0·03	−8·36	−15·48 to −1·24	0·02
MTR, per 10%	−2·66	−4·86 to −0·47	0·02	−1·96	−3·66 to −0·26	0·03	−2·06	−3·79 to −0·34	0·02
MFA, per 0·1mm [2]	−16·35	−102·55 to 69·84	0·70	−23·63	−87·59 to 40·33	0·46	−25·08	−90·29 to 40.14	0·44
For infarct size,%									
TTR, per 10%	8·92	−0·04 to 17·88	0·05	3·14	−2·95 to 9·22	0·30	3·54	−18·62 to 51·83	0·35
MTR‡, per 10%	1·01	−0·90 to 2·92	0·29	0·29	−0·85 to 1·43	0·61	0·31	−0·87 to 1·49	0·59
MFA⍰, per 0·1mm [2]	−21·43	−92·11 to 49·25	0·54	−10·49	−50·87 to 29·89	0·60	−10·09	−52·13 to 31·95	0·63
For MVO percentage,%									
TTR, per 10%	0·28	−0·37 to 0·94	0·39	0·09	−0·39 to 0·57	0·71	0·08	−0·41 to 0·56	0·76
MTR, per 10%	0·13	−0·03 to 0·29	0·10	0·07	0·01 to 0·13	0·02	0·07	0·01 to 0·13	0·02
MFA, per 0·1mm [2]	−0·02	−6·01 to 5·97	0·99	0·79	−1·04 to 2·63	0·39	0·31	−2·24 to 2·85	0·81
For GRS,%									
TTR, per 10%	−3·92	−9·46 to 1·63	0·16	−0·81	−5·34 to 3·71	0·72	−1·33	−5·91 to 3·25	0·56
MTR, per 10%	−1·82	−3·09 to −0·54	<0·01	−1·26	−2·28 to −0·23	0·02	−1·34	−2·35 to −0·32	0·01
MFA, per 0·1mm [2]	1·17	−50·19 to 52·53	0·96	4·65	−35·32 to 44·61	0·82	2·31	−37·91 to 42·53	0·91
For GCS,%									
TTR, per 10%	1·85	−0·80 to 4·50	0·17	0·45	−1·81 to 2·71	0·69	0·78	−1·43 to 2·96	0·48
MTR, per 10%	0·77	0·15 to 1·39	0·02	0·53	0·01 to 1·06	<0·05	0·58	0·08 to 1·08	0·03
MFA, per 0·1mm [2]	−0·89	−25·39 to 23·61	0·94	1·69	−17·89 to 21·26	0·86	2·32	−16·69 to 21·33	0·81
For GLS,%									
TTR¶, per 10%	−1·54	−4·82 to 1·75	0·35	−1·15	−3·93 to 1·63	0·41	−1·38 to 1·39	−4·15	0·32
MTR, per 10%	0·19	−0·34 to 0·72	0·47	0·07	−0·40 to 0·55	0·77	0·08	−0·41 to 0·57	0·75
MFA, per 0·1mm [2]	−1·91	−21·52 to 17·69	0·85	−0·90	−18·13 to 16·33	0·92	−0·59	−18·24 to 17·05	0·95

* Covariables included in the first multivariable model for each primary CMR outcome were as follows:.
1) for LVEF: peak cardiac troponin I (cTnI), peak N-terminal pro b-type natriuretic peptide (NT-proBNP), high-sensitivity C-reactive protein (Hs-CRP), and LVEF at admission;.
2) for infarct size: peak cTnI, peak NT-proBNP, Hs-CRP, estimated glomerular filtration rate (eGFR), and LVEF at admission;.
3) for MVO: peak cTnI and LVEF at admission;.
4) for GRS: peak cTnI, low density lipoprotein cholesterol (LDL-C), Hs-CRP, and LVEF at admission;.
5) for GCS: peak cTnI, Hs-CRP, and LVEF at admission;.
6) for GLS: peak cTnI and LVEF at admission.
† Based on the first multivariable models for each primary CMR outcome, age and sex were additionally adjusted to construct the second multivariable model for each primary CMR outcome.
‡ Casewise Diagnostics test recognised one outlier and 41 cases were finally included in the unadjusted, first and second adjusted model between MTR and infarct size.
⍰ Casewise Diagnostics test recognised one outlier and 41 cases were finally included in the unadjusted, first and second adjusted model between MFA and infarct size.
¶ Casewise Diagnostics test recognised two outliers and 40 cases were finally included in the unadjusted, first and second adjusted model between TTR and GLS.
CMR = cardiac magnetic resonance; GCS = global circumferential strain; GLS = global longitudinal strain; GRS = global radial strain; LVEF = left ventricular ejection fraction; MFA = minimal flow area; MTR = maximal thrombus-to-lumen ratio; MVO = microvascular obstruction; TTR = total thrombus-to-lumen ratio.

was the first difference between the current study and the previous ones. Second, we included only patients with a first-ever anterior STEMI. According to Torrent Guasp F's helical heart theory, basal transverse circumferential muscle shortens in pre-ejection phase and causes the temporary longitudinal lengthening of the heart, while the shortening of right-handed helical predominantly causes compression during ejection phase [33]. Romher et al. presented a right-handed to left-handed transition of dominant fiber and laminar structure in the anterior wall from septal to lateral wall [34]. Moreover, Stiermaier et al [35] reported different global strain changes in Takotsubo syndrome according to ballooning location. Thus, it is plausible that infarct location could impact myocardial deformation assessed by strain analysis, therefore, the significant differences of GRS and GCS but not GLS between patients with or without MTR>33% could be interpreted as a cohort feature. However, future studies are needed for further investigation.

Pathological characteristics of infarcted myocardia might serve as biological explanations between residual thrombus burden and myocardial deformation. On the one hand, MTR was significantly associated with MVO extent, which was in accordance with a recent study [36]. On the other hand, patients with higher MTR had numerically larger infarct size, while Napodano et al [27] reported a significant higher infarct size index in patients with angiographically defined large thrombus burden. Several differences should be noticed among studies. First, OCT provided intravascular evaluation of thrombus while angiographical assessment took into consideration haemodynamic factors. Second, both animal and human studies suggested an overestimation of infarct size by LGE imaging early after acute myocardial infarction [37,38] and infarct healing process could last over a year [39]. Although we performed CMR at 30 days after the index event, longer than 5 to 8 days after revascularization in Napodano's study, we could not deny that the enhancement of salvaged myocardium or no-infarcted extracellular volume could be unmeasured confounders.

Several study limitations should be mentioned. First, this is an observational study with prospectively enrolled patients and retrospectively collected data, therefore no causal relationship between residual thrombus burden and LV deformation could be established. Second, OCT examination is clinically restricted to patients with relative stable hemodynamic, thus selection bias could not be eliminated. Third, we enrolled only patients with a first anterior STEMI and this could also introduce selection bias. Forth, the population size was small and the results should be interpreted with caution. Limited sample size might increase the risk of random errors, Type I error (regarding those statistically significant results), and Type II error (regarding those statistically insignificant results). Therefore, we do not suggest direct generalization of these results for a broad acute myocardial infarction population and more future researches are needed for further investigation.

Conclusions

In current study, larger residual thrombus burden before stenting, as assessed by MTR, was associated with worse LV GRS and GCS but not GLS at one-month follow-up in patients with a first anterior STEMI after PPCI.

Contributors

Jinying Zhou and Shiqin Yu equally contributed to design, analysis and reporting of data and drafting of the manuscript. Chen Liu and Peng Zhou contributed to the study design and conduct. Zhaoxue Sheng, Jiannan Li and Runzhen Chen contributed to study conduct. Hongbing Yan and Shihua Zhao are responsible for the overall content as guarantors. All authors revised the manuscript critically for important intellectual content. All named authors who have accessed verified the underlying data.

Data sharing statement

All relevant data are presented in the manuscript and its supplementary material.

Declaration of Competing Interest

Prof Hongbing Yan received grants from Chinese Academy of Medical Sciences, National Natural Science Foundation of China, and Shenzhen Municipal Health Commission. Prof Shihua Zhao received grants from National Natural Science Foundation of China. The other authors declared none interests of conflicts.

Acknowledgements

None.

Funding

This work was funded by Chinese Academy of Medical Sciences Innovation Fund for Medical Sciences (2016-I2M-1−009), National Natural Science Foundation of China (81970308, 81930044, and 81620108015), Sanming Project of Medicine in Shenzhen (SZSM201911017), and Shenzhen Key Medical Discipline Construction Fund (No. SZXK001). All fundings had no involvement in any process of this study.

Supplementary materials

Supplementary material associated with this article can be found, in the online version, at doi:10.1016/j.eclinm.2021.101058.

References

[1] Stone GW, Peterson MA, Lansky AJ, Dangas G, Mehran R, Leon MB. Impact of normalized myocardial perfusion after successful angioplasty in acute myocardial infarction. J Am Coll Cardiol 2002;39:591–7.
[2] Niccoli G, Burzotta F, Galiuto L, Crea F. Myocardial no-reflow in humans. J Am Coll Cardiol 2009;54:281–92.
[3] Henriques JP, Zijlstra F, Ottervanger JP, et al. Incidence and clinical significance of distal embolization during primary angioplasty for acute myocardial infarction. Eur Heart J 2002;23:1112–7.
[4] Prati F, Pawlowski T, Gil R, et al. Stenting of culprit lesions in unstable angina leads to a marked reduction in plaque burden: a major role of plaque embolization? A serial intravascular ultrasound study. Circulation 2003;107:2320–5.
[5] de Waha S, Patel MR, Granger CB, et al. Relationship between microvascular obstruction and adverse events following primary percutaneous coronary intervention for ST-segment elevation myocardial infarction: an individual patient data pooled analysis from seven randomized trials. Eur Heart J 2017;38:3502–10.
[6] Svilaas T, Vlaar PJ, ICvd Horst, et al. Thrombus Aspiration during Primary Percutaneous Coronary Intervention. N Engl J Med 2008;358:557–67.
[7] Lagerqvist B, Frobert O, Olivecrona GK, et al. Outcomes 1 year after thrombus aspiration for myocardial infarction. N Engl J Med 2014;371:1111–20.
[8] Jolly SS, Cairns JA, Yusuf S, et al. Outcomes after thrombus aspiration for ST elevation myocardial infarction: 1-year follow-up of the prospective randomised TOTAL trial. Lancet 2016;387:127–35.
[9] Bhindi R, Kajander OA, Jolly SS, et al. Culprit lesion thrombus burden after manual thrombectomy or percutaneous coronary intervention-alone in ST-segment elevation myocardial infarction: the optical coherence tomography sub-study of the TOTAL (ThrOmbecTomy versus PCI ALone) trial. Eur Heart J 2015;36:1892–900.
[10] Higuma T, Soeda T, Yamada M, et al. Does residual thrombus after aspiration thrombectomy affect the outcome of primary PCI in patients with ST-segment elevation myocardial infarction? JACC 2016;9:2002–11.
[11] Panza JA, Ellis AM, HR Al-Khalidi, et al. Myocardial viability and long-term outcomes in ischemic cardiomyopathy. N Engl J Med 2019;381:739–48.
[12] Samady H, Elefteriades JA, Abbott BG, Mattera JA, McPherson CA, FJ. W. Failure to improve left ventricular function after coronary revascularization for ischemic cardiomyopathy is not associated with worse outcome. Circulation 1999;100:1298–304.
[13] Puntmann VO, Valbuena S, Hinojar R, et al. Society for cardiovascular magnetic resonance (SCMR) expert consensus for CMR imaging endpoints in clinical research: part I - analytical validation and clinical qualification. J Cardiovasc Magn Reson 2018;20:67.
[14] Garcia MJ, Kwong RY, Scherrer-Crosbie M, et al. State of the art: imaging for myocardial viability: a scientific statement from the American heart association. Circ Cardiovasc Imaging 2020;13:e000053.
[15] Kelle S, Roes SD, Klein C, et al. Prognostic value of myocardial infarct size and contractile reserve using magnetic resonance imaging. J Am Coll Cardiol 2009;54:1770–7.
[16] Gerber BL, Darchis J, le Polain de Waroux JB, et al. Relationship between transmural extent of necrosis and quantitative recovery of regional strains after revascularization. J Am Coll Cardiol Img 2010;3:720–30.
[17] Mewton N, Liu CY, Croisille P, Bluemke D, Lima JAC. Assessment of Myocardial Fibrosis With Cardiovascular Magnetic Resonance. J. Am. Coll. Cardiol. 2011;57:891–903.
[18] Taylor RJ, Moody WE, Umar F, et al. Myocardial strain measurement with feature-tracking cardiovascular magnetic resonance: normal values. Eur Heart J Cardiovasc Imaging 2015;16:871–81.
[19] Ibanez B, James S, Agewall S, et al. 2017 ESC Guidelines for the management of acute myocardial infarction in patients presenting with ST-segment elevation: the task force for the management of acute myocardial infarction in patients presenting with ST-segment elevation of the European Society of Cardiology (ESC). Eur Heart J 2018;39:119–77.
[20] von Elm E, Altman DG, Egger M, et al. The strengthening the reporting of observational studies in epidemiology (STROBE) statement: guidelines for reporting observational studies. Lancet 2007;370:1453–7.
[21] Levine GN, Bates ER, Blankenship JC, et al. 2015 ACC/AHA/SCAI focused update on primary percutaneous coronary intervention for patients with ST-elevation myocardial infarction: an update of the 2011 ACCF/AHA/SCAI guideline for percutaneous coronary intervention and the 2013 ACCF/AHA guideline for the management of ST-elevation myocardial infarction: a report of the American college of cardiology/american heart association task force on clinical practice guidelines and the society for cardiovascular angiography and interventions. Circulation 2016;133:1135–47.
[22] Tan Y, Sheng Z, Zhou P, et al. Plasma trimethylamine N-oxide as a novel biomarker for plaque rupture in patients with ST-segment-elevation myocardial infarction. Circ Cardiovasc Interv 2019;12:e007281.
[23] Sheng Z, Zhou P, Liu C, et al. Relationships of coronary culprit-plaque characteristics with duration of diabetes mellitus in acute myocardial infarction: an intravascular optical coherence tomography study. Cardiovasc Diabetol 2019;18:136.
[24] Zhou J, Sheng Z, Liu C, et al. Association between admission hyperglycemia and culprit lesion characteristics in nondiabetic patients with acute myocardial infarction: an intravascular optical coherence tomography study. J Diabetes Res 2020;2020:1–12.
[25] Tearney GJ, Regar E, Akasaka T, et al. Consensus standards for acquisition, measurement, and reporting of intravascular optical coherence tomography studies: a report from the international working group for intravascular optical coherence tomography standardization and validation. J Am Coll Cardiol 2012;59:1058–72.
[26] Subirana I, Sanz H, Vila J. Building bivariate tables: the compare groups package for R. J Stat Softw 2014;57:16.
[27] Napodano M, Dariol G, Al Mamary AH, et al. Thrombus burden and myocardial damage during primary percutaneous coronary intervention. Am J Cardiol 2014;113:1449–56.
[28] Kume T, Akasaka T, Kawamoto T, et al. Assessment of coronary arterial thrombus by optical coherence tomography. Am J Cardiol 2006;97:1713–7.
[29] Hu S, Yonetsu T, Jia H, et al. Residual thrombus pattern in patients with ST-segment elevation myocardial infarction caused by plaque erosion versus plaque rupture after successful fibrinolysis. J Am Coll Cardiol 2014;63:1336–8.
[30] Nucifora G, Muser D, Tioni C, Shah R, Selvanayagam JB. Prognostic value of myocardial deformation imaging by cardiac magnetic resonance feature-tracking in patients with a first ST-segment elevation myocardial infarction. Int J Cardiol 2018;271:387–91.
[31] Eitel I, Stiermaier T, Lange T, et al. Cardiac magnetic resonance myocardial feature tracking for optimized prediction of cardiovascular events following myocardial infarction. J Am Coll Cardiol Img 2018;11:1433–44.
[32] Reindl M, Tiller C, Holzknecht M, et al. Prognostic implications of global longitudinal strain by feature-tracking cardiac magnetic resonance in ST-elevation myocardial infarction. Circulation 2019;12:e009404.
[33] Torrent-Guasp F, Buckberg GD, Clemente C, Cox JL, Coghlan HC, Gharib M. The structure and function of the helical heart and its buttress wrapping. I. The normal macroscopic structure of the heart. Semin. Thorac. Cardiovasc. Surg. 2001;13:301–19.
[34] Rohmer Damien, Sitek Arkadiusz, Gullberg GT. Reconstruction and visualization of fiber and laminar structure in the normal human heart from ex vivo diffusion tensor magnetic resonance imaging (DTMRI) data. Invest Radiol 2007;42:777–89.

[35] Stiermaier T, Lange T, Chiribiri A, et al. Left ventricular myocardial deformation in Takotsubo syndrome: a cardiovascular magnetic resonance myocardial feature tracking study. Eur Radiol 2018;28:5160–70.
[35] Roule V, Schwob L, Lemaitre A, et al. Residual atherothrombotic burden after primary percutaneous coronary intervention and myocardial reperfusion-An optical frequency domain imaging study. Catheter Cardiovasc Interv 2020;96:91–7.
[36] Jablonowski R, Engblom H, Kanski M, et al. Contrast-enhanced CMR overestimates early myocardial infarct size: mechanistic insights using ECV measurements on day 1 and day 7. J Am Coll Cardiol Img 2015;8:1379–89.
[37] Hammer-Hansen S, Bandettini WP, Hsu LY, et al. Mechanisms for overestimating acute myocardial infarct size with gadolinium-enhanced cardiovascular magnetic resonance imaging in humans: a quantitative and kinetic study. Eur Heart J Cardiovasc Imaging 2016;17:76–84.
[39] Pokorney SD, Rodriguez JF, Ortiz JT, Lee DC, Bonow RO, Wu E. Infarct healing is a dynamic process following acute myocardial infarction. J Cardiovas Magnet Resonance 2012;14:62.